# The Hyperfine Structure and Nuclear Moments of $Pr^{141}$†

HIN LEW
*Division of Physics, National Research Council, Ottawa, Canada*
(Received April 20, 1953)

The hyperfine structure of the ground state of $Pr^{141}$ has been studied by the atomic beam magnetic resonance method. It has been established that the electronic ground state of Pr is $4f^36s^2$, $^4I_{9/2}$. Of the five hyperfine intervals arising from this electronic state and a nuclear spin of 5/2, the lowest two have been observed. They are $W(F=4)-W(F=3)=3708.05$ Mc/sec and $W(F=3)-W(F=2)=2782.25$ Mc/sec. If the hfs is assumed to be entirely due to an interaction between the $^4I_{9/2}$ state and the nucleus, the observed intervals may be expressed in terms of a magnetic dipole interaction constant $A$ and a nuclear electric quadrupole interaction constant $B$. It is found that $A=926.03\pm0.1$ Mc/sec and $B=-13.9\pm1.0$ Mc/sec. From these constants, the nuclear moments have been evaluated by means of approximate methods. The values obtained are

$$\mu=+3.8 \text{ nm}, \qquad Q=-0.054\times10^{-24} \text{ cm}^2.$$

## I. INTRODUCTION

THE experiment to be described in this paper represents the beginning of a program for the study of the rare earths by the atomic beam magnetic resonance method. The rare earths are of interest both on account of their atomic ground states and on account of their nuclear moments. For some of these elements the atomic ground states are not yet known. A determination of this characteristic through an investigation of the Zeeman effect should be of considerable assistance to spectroscopists in their analysis of the very complex spectra of these elements. Although the spin values of most of the rare earth nuclides have been reported, much remains to be done in the determination of their magnetic dipole moments and electric quadrupole moments. In view of the lack of success of the nuclear induction method in the case of the rare earths and in view of the difficulty of evaluating crystalline fields in the paramagnetic resonance method, it has been considered worth while to supplement and extend existing data by precise measurements of atomic hyperfine structures by the atomic beam method.

In 1929, White[1] observed that many of the lines of Pr II consisted of six hyperfine components. He was able to account for this observation on the basis that the $Pr^{141}$ nucleus had a spin of $(5/2)h/2\pi$. Later, Rosen, Harrison, and MacNally[2] studied the Zeeman effect of Pr II and succeeded in classifying many lines. They found that the lowest terms of Pr II were $f^3s$, $^{5,3}I$. From this result, it has been suggested[3] that the ground state of Pr I is probably $f^3s^2$, $^4I_{9/2}$. Thus, the present investigation started with a certain knowledge of the nuclear spin and a probable knowledge of the atomic ground state.

## II. THEORY

In the atomic beam magnetic resonance method, one studies the Zeeman effect of the hyperfine structure of the ground state or of low-lying metastable states of atoms. In a magnetic field an atom possessing an electronic angular momentum $J$ and a nuclear spin $I$ is usually described by a Hamiltonian of the form[4–6]

$$\mathcal{H}=A\mathbf{I}\cdot\mathbf{J}+BQ_{\text{op}}+g_J\mu_0\mathbf{J}\cdot\mathbf{H}+g_I\mu_0\mathbf{I}\cdot\mathbf{H}, \qquad (1)$$

where $Q_{\text{op}}$ stands for the operator

$$Q_{\text{op}}=\frac{3(\mathbf{I}\cdot\mathbf{J})^2+\frac{3}{2}(\mathbf{I}\cdot\mathbf{J})-IJ(I+1)(J+1)}{2IJ(2I-1)(2J-1)}.$$

$A$ and $B$ are interaction constants, and the respective terms in Eq. (1) represent the energy of interaction between the nuclear magnetic dipole moment and the magnetic field of the electrons and the energy of interaction between the nuclear electric quadrupole moment and the electric field of the electrons. The last two terms in the Hamiltonian represent the energy of the magnetic dipole moment of the electrons and of the nucleus, respectively, in the external field. The $g$ factors $g_J$ and $g_I$ are defined as the negative ratios of the electronic and nuclear magnetic dipole moments, respectively, in units of the Bohr magneton $\mu_0$ to the corresponding angular momenta in units of $h/2\pi$.

Theoretical expressions for the constants $A$ and $B$ in terms of fundamental atomic and nuclear quantities have been given by various authors. They will be considered later when we come to the evaluation of the nuclear quantities from the experimental results.

† Contribution No. 3038 from the National Research Council of Canada.

[1] H. E. White, Phys. Rev. **34**, 1397 (1929).

[2] Rosen, Harrison, and MacNally, Phys. Rev. **60**, 722 (1941).

[3] P. Schuurmanns, Physica **12**, 589 (1946); W. F. Meggers, Science **105**, 514 (1947).

[4] H. B. G. Casmir, *Interaction between Atomic Nuclei and Electrons* (Teyler's Tweede Genootschap, Haarlem, 1936).

[5] H. Kopfermann, *Kernmomente* (Akademische Verlagsgesellschaft, Leipzig, 1940; reprinted in U. S. by J. W. Edwards, Ann Arbor, 1945).

[6] Davis, Feld, Zabel, and Zacharias, Phys. Rev. **76**, 1076 (1949). Our notation differs from that of these authors in that we have used capital letters instead of small letters for the interaction constants $A$ and $B$. Capital letters have been used because they refer to the $^4I_{9/2}$ term arising from several electrons. The contributions of the individual electrons will be denoted by small letters.

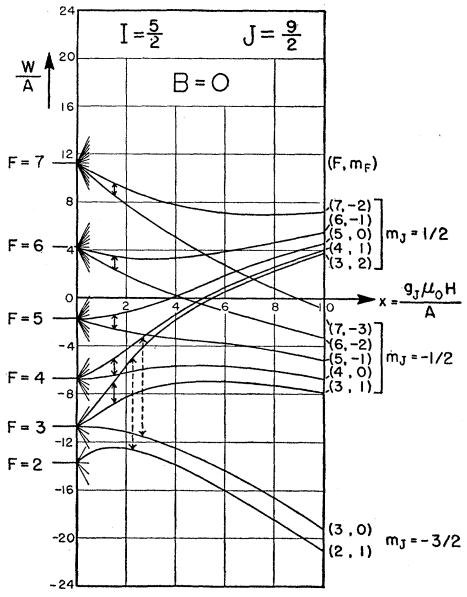


FIG. 1. Energy levels of an atom with $I=5/2$, $J=9/2$ in an external magnetic field, calculated for zero quadrupole interaction. Only those levels which have been observed in the present experiment are shown over the entire range of the parameter $x$.

The energy levels of an atom with the above Hamiltonian are simply the characteristic values of the matrix of the Hamiltonian. The matrix elements of the operators in the Hamiltonian may be found in many places in the literature.[7] In the $(I, J, F, m_F)$ representation, the matrix elements of $\mathbf{I}\cdot\mathbf{J}$ are particularly simple. They are independent of $m_F$ and are equal to $C/2$, where[8]

$$C=F(F+1)-J(J+1)-I(I+1).$$

Thus, in the absence of an external field, the characteristic values of the Hamiltonian are

$$W=A\frac{C}{2}+B\frac{\frac{3}{8}C(C+1)-\frac{1}{2}I(I+1)J(J+1)}{I(2I-1)J(2J-1)}. \quad (2)$$

These are the familiar hyperfine structure levels, each level being characterized by a given $F$, with the possible values of $F$ ranging from $I+J$ to $|I-J|$. If $B$ is zero, the spacings between these levels obey the interval rule.

In the presence of an external field, the energy levels cannot, in general, be expressed explicitly in terms of the various parameters. The secular determinant, in general, gives rise to equations which are of higher degree than the second. However, for very weak fields, first- or second-order perturbation theory may be applied to obtain approximate solutions. The first-order solution yields the result that each hyperfine level with quantum number $F$ splits up into $2F+1$ equally spaced magnetic levels with separations given by

$$\nu_F=g_J\frac{F(F+1)+J(J+1)-I(I+1)}{2F(F+1)}\mu_0H. \quad (3)$$

Transitions between adjacent magnetic levels belonging to a given value of $F$ are observable in the atomic beam magnetic resonance method and are called low-frequency (l.f.) transitions. It is obvious from Eq. (3) that if the $J$ and $g_J$ values of the electronic state are known, the spin $I$ may be determined by the observation of the low-frequency transitions. Conversely, if $I$ is already known, $J$ and $g_J$ may be determined. This will be illustrated below for the case of Pr. It is even possible to determine all three quantities $I$, $J$, and $g_J$, provided there is a sufficient number of $F$'s and therefore $\nu_F$'s.

In the present experiments, $J$ was not known initially. Various values of $J$ were assumed, and energy level diagrams of the corresponding hyperfine structures constructed in order to see what levels satisfied the refocusing conditions of the experiment and were therefore observable. In Fig. 1 is shown such a diagram for $I=5/2$ and $J=9/2$, this value of $J$ being the one eventually found for Pr. To avoid unnecessary confusion, only some of the levels have been shown over the entire range of the parameter of the abscissa. These levels have been determined by numerical solution of the secular determinant of the Hamiltonian, Eq. (1), with $B$ and $g_I$ set equal to zero and the whole expression divided through by $A$. In other words, they are the characteristic values of

$$\mathcal{H}'=\mathcal{H}/A=\mathbf{I}\cdot\mathbf{J}+xJ_z, \quad (4)$$

where $x=g_J\mu_0H/A$ and $J_zH=\mathbf{J}\cdot\mathbf{H}$ if $\mathbf{H}$ is in the $z$ direction.

At weak fields, the low frequency lines are, by Eq. (3),

$$\begin{aligned}&\nu_7=(9/14)g_J\mu_0H, \quad \nu_4=(9/10)g_J\mu_0H,\\ &\nu_6=(29/42)g_J\mu_0H, \quad \nu_3=(7/6)g_J\mu_0H,\\ &\nu_5=(23/30)g_J\mu_0H, \quad \nu_2=(11/6)g_J\mu_0H.\end{aligned} \quad (5)$$

The ratios of these low frequency lines depend only on $I$ and $J$ and not on $g_J$ or the term type. It can be easily verified that for $I=5/2$, no value of $J$ other than $9/2$ will give rise to a set of low frequency lines which are related in the above proportions. Thus, by observing the relative frequencies of a set of low frequency lines, one may determine $J$ uniquely. From the absolute frequencies, one may then calculate $g_J$, the Landé $g$ factor of the electronic state. The association of a term type with a given $g_J$ will, of course, depend on the electronic coupling assumed and, even with a given coupling, may not be unique. Thus, other considerations will, in general, need to be brought in for a unique identification of the term type.

[7] See E. U. Condon and G. H. Shortley, *Theory of Atomic Spectra* (Cambridge University Press, Cambridge, 1935).

[8] Authors are divided between the symbols $K$ and $C$ for this expression, and we have chosen $C$ to conform with the usage in molecular spectroscopy.

## III. EXPERIMENTAL PROCEDURE AND APPARATUS

### (a) The Over-All System

The present atomic beam magnetic resonance apparatus is patterned after those of the Molecular Beam Laboratory of the Massachusetts Institute of Technology.[9,10] The essential dimensions and the locations of the various components are shown in Fig. 2. There are the usual two inhomogeneous deflecting fields $A$ and $B$ on either side of a homogeneous field $C$ where transitions take place. The magnetic field gradients in the $A$ and $B$ regions are parallel to each other and in the same direction, an arrangement first used by Zacharias[11] in the study of $K^{40}$. Atoms which do not undergo transitions in traversing the magnetic fields are swept away from the detector which lies on the neutral axis of the beam. Only those atoms are redeflected back on to the detector which undergo transitions between states with effective magnetic moments of the opposite sign in the $A$ and $B$ fields. This special "refocusing" condition restricts the number of observable transitions to considerably less than that permitted by the selection rules. This apparent disadvantage, however, is outweighed by the advantage that there is no large background of atoms striking the detector when there is no transition.

The loop in the $C$ field through which radio-frequency power is sent for the inducement of transitions is a vertical hairpin about 1.5 inches high which produces an oscillating magnetic field directed mainly parallel to the atomic beam and about $\frac{3}{8}$ inch in extent in this direction. Another loop of wire mounted close to this one but out of the way of the beam is used to pick up the field radiated by the first loop. By rectifying the rf energy with a crystal rectifier and measuring the resultant current in a microammeter, some indication is obtained of the power that is in the transition region.

Caesium atoms are used to measure the field strength in the $C$ region. The particular line used is $(F=4, m_F=-3)\rightarrow(F=4, m_F=-4)$ which, at weak fields, is related to the field strength through the first-order approximation.

$$\nu=0.35H \text{ Mc/sec}, \tag{6}$$

where $H$ is in gauss.

The widths of the various slits are as follows: oven 0.004 inch, collimator 0.006 inch, ionizer or detector 0.015 inch. The first obstacle wire is 0.010 inch in diameter and the second 0.008 inch in diameter. The presence of two obstacle wires instead of the usual one will be explained below in connection with the determination of the sign of the magnetic dipole interaction constant.

The electron multiplier for the detection of ions is a 15-stage secondary electron emission multiplier with

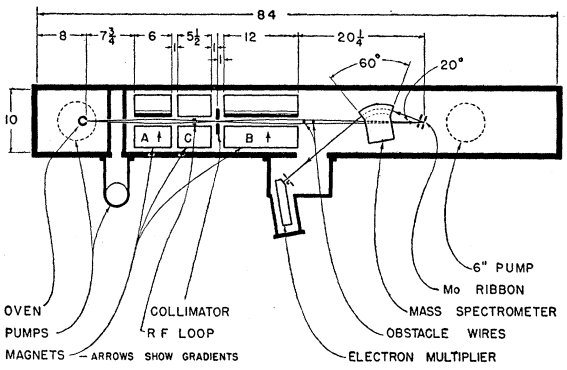


FIG. 2. Diagram of atomic beam magnetic resonance apparatus showing locations of components. All dimensions are in inches.

dynodes of beryllium-copper. The shapes of the electrodes and their preparation are exactly as described by Allen.[12]

### (b) The Vacuum System

The vacuum housing is a box of square cross section 10 in.×10 in. inside dimensions and 84 in. long. The walls are of rolled brass plate, 1 in. thick on top and $\frac{3}{4}$ in. thick on the other three sides. The joints between the plates are grooved, screwed together, and soft soldered. The top plate is planed smooth and flat after assembly, since it is used as the reference plane for the components which go into the vacuum system. As is the case with the instruments at the Massachusetts Institute of Technology, all the components are suspended from brass plates which lie over rectangular ports in the reference plane. The vacuum seal between these brass mounting plates and the reference surface is accomplished by vacuum grease and Apiezon Q wax. The ends of the box are closed by flat brass plates and again made vacuum tight with Apiezon Q wax. All windows and pump connections to the box are made through O-ring gaskets.

The three chambers of the vacuum housing are individually evacuated, the oven and detector chambers by 6-in. diameter oil diffusion pumps and the isolation chamber by a 4-in. diameter pump. Gate valves and water-cooled baffles are provided in the connections between the pumps and the box. Furthermore, a small gate valve is provided between the oven chamber and the isolation chamber to permit air to be let into the oven chamber without affecting the vacuum in the rest of the system. The diffusion pumps are backed by two oil booster pumps and these in turn by two mechanical pumps. In operation, one small mechanical pump is sufficient to back the boosters. When pumping the system down from atmospheric pressure, however, the other larger mechanical pump is brought into play, first for roughing out the system and then for backing the diffusion pumps until a high degree of vacuum is reached. Liquid air traps are introduced into the three

[9] Davis, Nagle, and Zacharias, Phys. Rev. **76**, 1068 (1949).
[10] Eisinger, Bederson, and Feld, Phys. Rev. **86**, 73 (1952).
[11] J. R. Zacharias, Phys. Rev. **61**, 270 (1942).
[12] J. S. Allen, Rev. Sci. Instr. **18**, 739 (1947).

TABLE I. Data on magnets.

| *A* and *B* magnets | *A* | *B* |
|---|---|---|
| Length | 6 | 12 inches |
| Separation of equivalent 2-wire system | 0.250 | 0.750 inch |
| Gap at apex | 0.0937 | 0.125 inch |
| Number of turns | 39.5 | 28 |
| Field *H* | 208 | 111 gauss/amp |
| Gradient | 3.15 *H* | 1.05 *H* gauss/cm |
| *C* magnet | | |
| Length | $5\frac{1}{2}$ inches | |
| Gap | 0.250 inch | |
| Number of turns | 36 | |
| Field | 67 gauss/amp | |
| Mass spectrometer magnet | | |
| Radius of curvature | 5 inches | |
| Angle of sector | 60 degrees | |
| Gap | $\frac{1}{2}$ inch | |
| Number of turns | 40 | |

chambers through side ports. A vacuum of better than $10^{-6}$ mm Hg is easily obtainable in the detector chamber. The pressure in the oven chamber depends on the evolution of gas from the oven and is usually $10^{-5}$ mm Hg or less. The pressure in the isolation chamber is usually around $10^{-6}$ mm Hg.

### (c) The Magnets

All the magnets are made of Armco magnet iron with windings of copper tubing insulated with Fiberglas sleeving. Their essential dimensions and characteristics are given in Table I.

The *A* and *B* magnets are of conventional design,[13] the pole pieces being shaped to give a field distribution in the gap which is equivalent to that of two parallel wires carrying equal currents in opposite directions. The pole pieces are reversible without disturbing the yokes so that the gradients in the *A* and *B* fields may be made parallel or antiparallel. With the geometry as shown in Fig. 2 and magnet characteristics as given in Table I, the refocusing condition for atoms with equal and opposite effective magnetic moments in the *A* and *B* fields is that the gradient in the *B* field shall be 0.32 times that in the *A* field. Typical energizing currents for achieving this are 30 amperes in *A* and 55 amperes in *B*.

The *C* magnet is of the simplest possible construction being composed entirely of rectangular pieces bolted together. The gap faces are ground smooth and flat and separated by precision spacers. For the present experiment, no attempt had been made to homogenize the field through shimming.

The mass spectrometer magnet is of the familiar 60° sector type.

### (d) The Ovens

Two ovens are used in the present experiment, one for the generation of a beam of Pr atoms and the other one for a beam of Cs atoms. The two ovens are mounted in such a way that either one may be brought into the proper operating position simply and accurately without disturbing the vacuum in the oven chamber. The arrangement is shown in Fig. 3. The two ovens are mounted on the underside of a rotatable platform which is made vacuum tight with respect to its mounting plate by means of an O-ring. The angular position of the platform is accurately located through micrometer stops, and it has been found that the positions of the ovens may be set to about 0.001 inch.

The cell used for the vaporization of Pr is essentially a thin-walled molybdenum cylinder with a slit cut longitudinally in the wall. The unit is machined from $\frac{3}{8}$-inch solid molybdenum rod into the form shown in the figure. The thin-walled section is $\frac{1}{4}$ inch in inside diameter and $\frac{5}{16}$ inch in outside diameter, and the slit in it is 0.004 inch by $\frac{1}{8}$ inch. The unit is clamped by its lower stem between two blocks of copper which are in thermal and electrical contact with the bottom of the water-cooled radiation shield surrounding the unit. The top end of the cell, i.e., the stem of the cap that closes the cylindrical chamber, protrudes through the radiation shield and makes contact with a water-cooled copper block which is electrically insulated from the rest of the oven assembly. Electrical power is applied between this electrode and the radiation shield by way of the tubes which lead cooling water to these parts. The praseodymium metal to be vaporized, instead of being placed in direct contact with the molybdenum, is contained in a $ThO_2$ crucible. This greatly reduces the chances of the oven slit being clogged by the molten metal. A current of about 240 amperes at 10 volts is required to bring the oven to the operating temperature of 2000°K (1570°C brightness temperature at a wavelength of 0.65$\mu$).

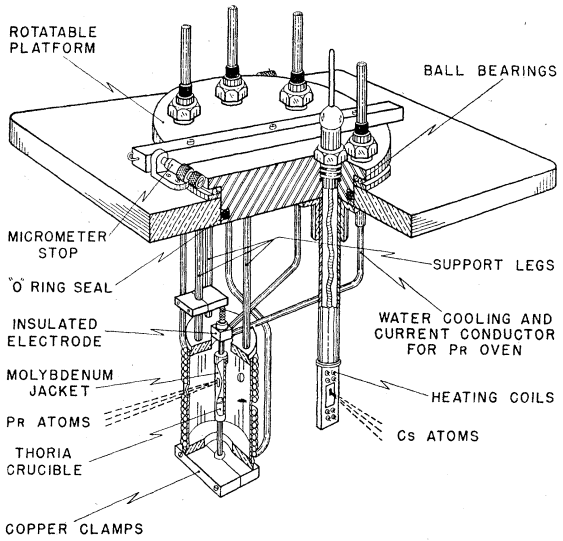


FIG. 3. The Pr and Cs ovens shown mounted on rotatable platform for simple and accurate interchange of positions.

[13] Millman, Rabi, and Zacharias, Phys. Rev. **53**, 384 (1938).

The oven for the production of a Cs beam consists of an iron cell of square cross section $\frac{1}{4}$ in.$\times\frac{1}{4}$ in.$\times\frac{7}{8}$ in. with a longitudinal slit in one face 0.004 in.$\times\frac{1}{8}$ in. This fits into a rectangular hole in a block of iron in which are imbedded some molybdenum heating coils. A charge of Na metal and CsCl in the cell yields a very steady beam of Cs atoms when the oven is raised to a temperature of about 200°C.

### (e) The Ionizer

For the detection of the neutral atoms of an atomic beam, the atoms may be ionized by the familiar surface ionization method. Because of its low ionization potential of 3.9 volts, Cs can be ionized by any of a large number of metals by this process. However, considerable difficulty was experienced in finding a suitable ionizer for Pr. Of the various refractory elements tried, including Pt, W, Cb, and Mo, molybdenum was found to be the best, even though it suffered from two serious limitations. The first limitation is its low efficiency.The work function $\phi$ of Mo is 4.27 ev,[14] while the ionization potential $I$ of Pr is approximately 5.76 ev.[15] With the Mo ribbon at a temperature of 2070°K, which is experimentally found to be the temperature of best compromise between ionization efficiency and long life, the probability of ionization, as given by $\exp[(\phi-I)/kT]$ is $2\times10^{-4}$. This low efficiency is still usable, however, by using a high enough incident beam intensity and measuring the ion intensity with an electron multiplier and a pulse counting system. The more serious defect of Mo as a surface ionizer is that the re-emission of Pr from its surface as ions does not take place instantaneously. The delay between the striking of the neutral atom on the surface and its re-emission as an ion varies from one or two seconds when the Mo ribbon is at 2160°K to about 30 seconds at 1870°K. At the higher temperatures, the ribbon, which is under slight tension to keep it taut, easily breaks and also diminishes in size rapidly through evaporation. The most practical operating temperature has been found to be about 2070°K, at which temperature the time delay is about 3 seconds. It is obvious that, with this time constant, the search for narrow transition lines over a wide frequency range can become extremely tedious.

The molybdenum ribbon used in the present experiments measured 0.015 inch wide by 0.002 inch thick and is of commercial purity. Before such a ribbon can be used as a detector of Pr, it must be cleaned by prolonged heating in vacuum. It seems that the Mo is contaminated by many oxides including those of the rare earths. When a new ribbon is first installed in the ionizer assembly and brought up to about 2070°K, it emits ions copiously over a wide range of masses. One of these masses is of mass number 157 and is probably PrO. As long as this impurity is present, it is found that a Pr atom striking the surface is not re-emitted as $Pr^+$ but as an ion of mass 157 which presumably is $PrO^+$. This behavior itself would not be objectionable, for the atomic beam would be detected thereby anyway, if it were not for the fact that the background from the wire itself at this same mass number is unsteady, and its magnitude prevents the observation of weak transitions that would otherwise be observed. In order to remove this impurity, it has been found sufficient to maintain the ribbon at a temperature of about 2000°K for about 12 hours. The ribbon then re-emits Pr atoms as $Pr^+$ with a reasonably steady and tolerably low background.

Of the other materials that were tried as ionizers, tungsten was found to have a time delay several times greater than that of Mo. Columbium, on the other hand, had a shorter delay, but its ionization efficiency was lower because of its lower work function (3.99 ev). Platinum with its high work function of 5.1 ev would probably have made an efficient ionizer if it had not been for the fact that, because of its low melting point, it broke too easily at the temperatures necessary for the re-evaporation of Pr.

### (f) Oscillators and Frequency Meters

A variety of oscillators was used to cover the wide range of frequencies encountered in the present study. For the $\Delta F=0$ lines, the following oscillators were used: General Radio Type 1001-A (5 kc/sec–50 Mc/sec), General Radio Type 1208-A (65 Mc/sec–500 Mc/sec), Airborne Instruments Laboratory Type 124A Power Oscillator (300 Mc/sec–2500 Mc/sec). For the $\Delta F=1$ lines, Sperry reflex klystrons were used, the 2K41 for the 2782 Mc/sec line, and the 2K42 for the 3708 Mc/sec line. Higher frequency lines of the hyperfine structure were searched for unsuccessfully with the 2K43 and 2K44.

Frequencies below 100 Mc/sec were measured with a General Radio Type 620-A Heterodyne Frequency Meter and Calibrator. The accuracy of this instrument is 1 part in $10^4$ or better. Frequencies above 100 Mc/sec were measured with a General Radio Type 720A Heterodyne Frequency Meter in conjunction with a General Radio Type 1110-A Interpolating Frequency Standard. The crystal oscillator in the latter has been checked against standard transmissions from station WWV and found to be correct to 1 part in $10^5$ or better.

## IV. RESULTS

### (a) $\Delta F=0$, $\Delta m_F=\pm1$ Transitions

At the outset of the present experiments, when the atomic ground state of Pr was not known, a general search was made for transitions between magnetic levels belonging to the same $F$. These transitions were sought at low fields of a few tens of gauss, i.e., in the Zeeman region where linear relations of the type Eq. (3) held to a percent or better. The $C$ field was held

[14] H. B. Michaelson, J. Appl. Phys. **21**, 536 (1950).
[15] L. Rolla and G. Piccardi, Phil. Mag. **7**, 286 (1929).

TABLE II. Low frequency lines.

| Observed Pr lines | | | | | | Theoretical lines for $I=5/2$, $J=9/2$ | | |
|---|---|---|---|---|---|---|---|---|
| At 28.37 gauss | | At 56.31 gauss | | At 83.85 gauss | | Frequency in units $g_J\mu_0 H$ | | Relative to $(F=6)$ |
| Freq., Mc/sec | Rel. freq. | Freq., Mc/sec | Rel. freq. | Freq., Mc/sec | Rel. freq. | | | |
| 18.67 | 0.932 | 37.08 | 0.930 | 55.19 | 0.931 | $F=7$ | 9/14 | 0.9310 |
| 20.03 | 1.000 | 39.88 | 1.000 | 59.28 | 1.000 | $F=6$ | 29/42 | 1.0000 |
| 22.26 | 1.111 | 44.26 | 1.110 | 65.88 | 1.111 | $F=5$ | 23/30 | 1.1103 |
| 26.06 | 1.301 | 51.90 | 1.301 | 77.23 | 1.303 | $F=4$ | 9/10 | 1.3034 |
| 33.65 | 1.679 | 67.09 | 1.682 | 99.58 | 1.680 | $F=3$ | 7/6 | 1.6896 |
| | | | | | | $F=2$ | 11/6 | 2.6552 |

constant, while the frequency in the rf loop was varied over a reasonably wide range, say 50 kc/sec to 50 Mc/sec. The magnitude of the $C$ field was determined by the low frequency transition of $Cs^{133}$. After the proper experimental conditions (oven temperature, ionizer material, and rf field strength) had been found for the detection of transitions, five $\Delta F=0$, $\Delta m_F=\pm 1$ transitions were observed in Pr at a given value of the $C$ field. A series of readings at $C$ fields of 28.37 gauss, 56.31 gauss, and 83.85 gauss are shown in Table II. These magnetic fields correspond to low frequency transitions in $Cs^{133}$ of 10.0 Mc/sec, 20.0 Mc/sec, and 30.0 Mc/sec, respectively. Each reading represents a single setting of the oscillator on the estimated peak of the line. The width of each line is about 0.2 Mc/sec, and, therefore, the peaks are probably no more accurately located than to 0.05 Mc/sec. At each field strength, the observed frequencies are reduced to a set of relative values, as shown in the table. The line with the second lowest frequency was chosen as the reference line in this relative scale, because it was found to be the strongest and, therefore, the most accurately measurable.

Assuming that these $\Delta F=0$, $\Delta m_F=\pm 1$ transitions all belonged to the same hyperfine multiplet, various values of the electronic angular momentum $J$ were assumed and, with $I=5/2$, the theoretical relative frequencies of the possible low frequency lines calculated by Eq. (3). Only for $J=9/2$ was any agreement found between the calculated relative frequencies and the observed relative frequencies. This agreement is seen in Table II where the calculated values are shown in the last two columns. Within the accuracy of the measurements and the validity of the first-order approximation, the agreement may be considered to be exact. We may conclude that the $J$ value of the electronic state under study is almost certainly 9/2. All subsequent observations are in agreement with this $J$ value. We shall, therefore, in our discussions consider this $J$ value as being correct.

From Fig. 1 we may identify the magnetic quantum numbers of the levels involved in the observed transitions. The gradients of the $A$ and $B$ fields were set, in the observations, to refocus equal and opposite magnetic moments. Assuming that the strength of these fields are sufficiently high so that the Pr atoms are in the Paschen Back region while going through the deflecting fields, then, remembering that the magnetic quantum number $m_F$ may change by unity only, the only observable transitions are those between levels with strong field quantum number $m_J=\frac{1}{2}$ and $m_J=-\frac{1}{2}$. This allows us to deduce immediately that the observed transitions were $(7, -2)\rightarrow(7, -3)$, $(6, -1)\rightarrow(6, -2)$, $(5, 0)\rightarrow(5, -1)$, $(4, 1)\rightarrow(4, 0)$, $(3, 2)\rightarrow(3, 1)$. These are shown by the solid arrows in the figure. The reason why no l.f. transition belonging to $F=2$ was observed is simply that the magnetic levels of $F=2$ all have negative $m_J$, while at least one positive $m_J$ is necessary for refocusing.

As mentioned above, the $(6, -1)\rightarrow(6, -2)$ line was found to be considerably stronger than the others. The reason for this was not understood until the hyperfine structure interval factor $A$ had been found. It was then realized that the magnetic fields of 5500 gauss used in the $A$ and $B$ regions corresponded to $x=g_J\mu_0 H/A=6$ and that, at this value of $x$, the Pr atoms were not in the Paschen-Back region where their effective magnetic moments assumed the limiting values $-m_J g_J \mu_0$. As may be seen from Fig. 1, the effective magnetic moments at $x=6$ may be greater or less than those in the Paschen-Back region. The initial and final levels of all the observed low frequency transitions except $(6, -1)\rightarrow(6, -2)$ do not have equal and opposite slopes in this intermediate field region. Since the $A$ and $B$ fields were set to refocus equal and opposite magnetic moments, only the line belonging to $F=6$ was properly refocused. The others were improperly refocused and hence were of lower intensity.

Once $J$ has been found from the relative frequencies of the observed transitions and the identification of the latter has been accomplished, the Landé $g$ factor of the fine structure state may be calculated from the absolute frequencies. Using the observations at 28.37 gauss shown in Table II and observations at lower fields not shown, we find from Eq. (5) $g_J=0.731\pm 0.004$.[16] The large error in this value is partly due to the inaccuracy

[16] The value of $0.727\pm 0.005$ quoted in a preliminary note [H. Lew, Phys. Rev. **89**, 530 (1953)] differs from this value, because in the previous value the magnetic field $H$ was calculated from the Cs frequency by means of the first-order relation, Eq. (6). In the present case, $H$ has been calculated by means of the exact Breit-Rabi formula, using the Cs constants given by P. Kusch and H. Taub [Phys. Rev. **75**, 1477 (1949)].

on the measurements and partly due to the inaccuracy of the first-order expressions, Eq. (5). A better value may be found by using second-order expressions for the low-frequency lines which contain the magnetic dipole interaction constant $A$ determined later in the experiment. With this little refinement, we find, on simply averaging the results of the five levels, $g_J=0.731 \pm 0.002$, i.e., the average value is unchanged but the limits of error are reduced. The effect of $g_I$ has been neglected in these calculations for the limited accuracy of the measurements does not warrant its inclusion.

Knowing $J$ and $g_J$ for the state under study, we may search the tables for likely term types. If we assume that Russell-Saunders coupling holds for the state, we find that the term type with $J=9/2$, and $g_J$ nearest 0.731 is $^4I_{9/2}$. For pure Russell-Saunders coupling, this term type has a $g$ value of 0.727. The observed deviation of $\frac{1}{2}$ percent from the extreme Russell-Saunders value is not surprising, considering the complexity of atomic spectra in the rare earth region of the periodic system. A $^4I_{9/2}$ ground term implies, according to Hund's rules, an $f^3$ or $f^3s^2$ electron configuration. An $f^3s^2$, $^4I_{9/2}$ ground term is very plausible in view of the known ground terms, $f^3s$, $^{3,5}I$, of Pr II, as mentioned in the introduction.

Further evidence that the state under study is $^4I_{9/2}$ comes from our observation of low-frequency lines which may be ascribed to $^4I_{11/2}$. If the state under investigation is indeed $^4I_{9/2}$ and is the ground state, then there should exist metastable states $^4I_{11/2}$, $^4I_{13/2}$, $^4I_{15/2}$. The low-frequency lines belonging to the hfs of $^4I_{11/2}$ may be calculated by means of Eq. (3), using $g_J(^4I_{11/2})=0.965$, the value corresponding to extreme Russell-Saunders coupling. Such lines were sought and found, except that a $g_J$ of 0.970 fitted the observations better than 0.965. The intensities of these lines were about 40 percent of those belonging to $^4I_{9/2}$. This is in agreement with the relative populations of the two states at 2000°K, if the two states are separated by the 1450 $cm^{-1}$ which we have estimated below.

### (b) $\Delta F=1$, $\Delta m_F=\pm 1$ Transitions

When the magnitudes of the hfs intervals are completely unknown, it is generally impractical to search for them with a continuous sweep over a wide rf spectrum. It is customary to make an estimate of the hfs constant $A$ through the low-frequency lines. Explicit expressions for the dependence of the observable low frequency transitions on $A$ are not obtainable in cases where $I$, $J>\frac{1}{2}$. One must resort to approximate perturbation expressions or to numerically computed detailed plots of the energy levels, such as those shown in Fig. 1. We have followed the latter method. It will be noticed that $A$ enters into both the ordinate and the abscissa. Only for the correct choice of $A$ will an observed low frequency line fit into the energy level diagram at the value of $x$ calculated for the assumed $A$ and for the observed magnetic field $H$. For our low-frequency line, we chose $(6, -1)\rightarrow(6, -2)$, since it was the strongest for reasons already mentioned. It was measured accurately at 1000 gauss, and its frequency was found to be 723.9 Mc/sec. Using $g_J=0.727$, the theoretical Landé $g$ value for $^4I_{9/2}$, we found a value for $A$ of approximately 830 Mc/sec. This turned out to be about 12 percent lower than the correct value which was eventually found. On examining our original calculations, we discovered that if we had taken for $g_J$ the value 0.731 which was contained in our low frequency observations, we would have come to within 2 or 3 percent of the correct value of $A$. We were fortunate in finding a $\Delta F=\pm 1$ transition, despite the poor estimate.

The first high-frequency line was found at around 3320 Mc/sec at a $C$ field of approximately 570 gauss. This was followed down to as low a field as possible, the last measurement taken being at appromately 1 gauss. The measurements between zero and 30 gauss are shown in Fig. 4. The sizes of the circles in the figure do not represent the probable errors in the measurements. These are less than 0.1 Mc/sec and cannot be shown in the scale of the figure. By plotting the observations on a large scale and extrapolating graphically to zero field, we find a frequency of $2782.25 \pm 0.05$ Mc/sec. Furthermore, the field dependence of this line at zero field is $0.51 \pm 0.01$ Mc/sec-gauss. This slope enables us to identify the line unambiguously as the $(F=3, m_F=2) \rightarrow (F=2, m_F=1)$ transition (assuming $A$ positive, as shown below). The theoretical slopes of the energy levels at zero field are given rigorously by the first-order expressions, and, for the $(3, 2)\rightarrow(2, 1)$ transition, the theoretical slope is $0.500\ g_J\mu_0$ or, using $g_J=0.731$ and $\mu_0=1.400$ Mc/sec-gauss, it is 0.512 Mc/sec-gauss. There is no other transition between $F=3$ and $F=2$ which has a theoretical slope within 33 percent of this

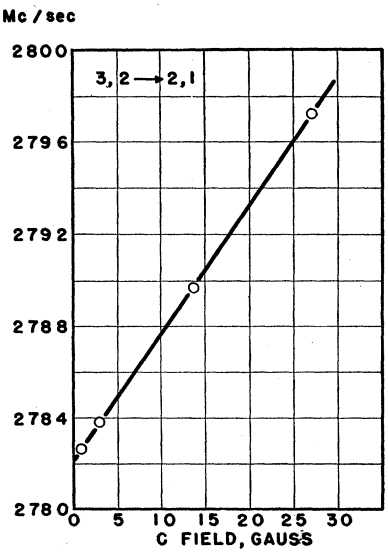


FIG. 4. (3,2)→(2,1) transition in Pr plotted against $C$ field.

value. The closest is $(3, -1)\rightarrow(2, -1)$ which has a theoretical slope of 0.67 $g_J\mu_0$ or 0.685 Mc/sec-gauss. This line can be safely excluded, not only because of its slope but also because of its unobservability in the apparatus. The possibility of the observed line belonging to the hyperfine interval $(F=4)\rightarrow(F=3)$ may also be excluded by slope considerations.

Assuming that the interval rule held approximately for the hfs of Pr, a search was next made for transitions between $F=4$ and $F=3$ at frequencies in the vicinity of 4/3 of 2782 Mc/sec. One was duly found at 3730 Mc/sec at a $C$ field of about 23 gauss. This was followed down to 1 gauss and extrapolated to zero field. The zero field frequency was 3708.05±0.05 Mc/sec. From its field dependence at zero field, the line was positively identified as $(4, 1)\rightarrow(3, 0)$. The results are shown in Fig. 5.

Search for further lines belonging to the same hyperfine intervals as the above two and for lines belonging to higher intervals was unsuccessful. The lack of success in the latter aspect may be explained on the basis of insufficient microwave power in the transition region. For a $F=5\rightarrow F=4$ transition, for instance, rf power of frequencies around 4635 Mc/sec or wavelengths around 6.57 cm was needed. The output of a 2K43 klystron was coupled to the rf loop in the $C$ field through a coaxial line and a single tuning stub. The energy picked up by the monitoring loop in the $C$ region indicated very little power there. This was probably due to the crudeness of the electrical matching system. Unfortunately, there was no equipment on hand to permit an attempt at better matching. Aside from the indication provided by the monitoring loop, another indication that our rf system was inefficient at higher frequencies was the fact that the 3708-Mc/sec transition was several times weaker than the 2782-Mc/sec transition.

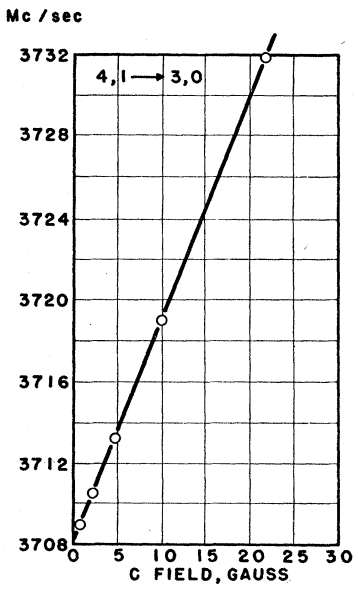


FIG. 5. (4,1)→(3,0) transition in Pr plotted against $C$ field.

With regard to the question why no other transitions between $F=4$ and $F=3$ and between $F=3$ and $F=2$ were found, a detailed examination of the energy levels showed that no other transitions were favored either by the selection rules or by the refocusing condition. Between $F=3$ and $F=2$, the only transitions which are allowed by the selection rules and by the refocusing condition that $m_J$ must change in sign are $(3, 3)\rightarrow(2, 2)$, $(3, 2)\rightarrow(2, 2)$, and $(3, 2)\rightarrow(2, 1)$. The last one has been observed. The first one is not favorable to refocusing because the $(2, 2)$ level has an effective magnetic moment of nearly zero at $x=6$. The second one has the same unfavorable characteristic. In addition, it is a $\Delta m_F=0$ transition and would have required a polarization of the rf field perpendicular to that actually used. The same arguments apply to $(4, 2)\rightarrow(3, 1)$, $(4, 1)\rightarrow(3, 1)$, and $(4, 1)\rightarrow(3, 0)$. Thus, we observed all the lines which were allowed by the selection rules and the experimental conditions.

If the hyperfine structure of the $^4I_{9/2}$ state under study is not appreciably perturbed by higher levels of the same multiplet, we may express our observations in terms of the two constants $A$ and $B$ appearing in Eq. (2):

$$4A-(17B/60)=3708.05\pm0.05 \text{ Mc/sec},$$

$$3A-(3B/10)=2782.25\pm0.05 \text{ Mc/sec}.$$

Hence,

$$A=926.03\pm0.10 \text{ Mc/sec}, \quad B=-13.9\pm1 \text{ Mc/sec},$$

$$B/A=-0.0150.$$

### (c) The Sign of $A$

So far in the interpretation of our observations, we have tacitly assumed that the magnetic dipole interaction constant $A$ is positive. An internally consistent interpretation could just as well have been obtained for a negative $A$. To determine the sign of $A$, we have examined the trajectories of the atoms under special refocusing conditions in the manner outlined by Davis, Feld, Zabel, and Zacharias.[6] When the gradients in the $A$ and $B$ deflecting regions are such as to refocus equal and opposite magnetic moments, atoms which have undergone transitions either through the absorption of a quantum of energy or through the stimulated emission of a quantum of energy strike the detector in equal numbers. Their trajectories, however, are different. One group follows a sigmoid path which takes them around one side of the obstacle wire, and the other group follows a path which takes them around the other side of the obstacle wire. This symmetry is lost, however, when the $A$ and $B$ fields are set to refocus atoms which have effective magnetic moments in the two regions differing not only in sign but also in magnitude. In Fig. 6(a), we show the energy levels involved

in the 2782-Mc/sec line for $A$ assumed positive and in Fig. 6(b) the corresponding levels for $A$ assumed negative. The vertical dotted lines indicate the magnetic fields which existed in the $A$ and $B$ deflecting regions in the trajectory exploration. Under these conditions, the gradients are such that only the transition indicated by the solid arrow in either case is refocused. The accompanying transition indicated by the dotted arrow is not refocused, because the effective magnetic moments of the initial and final levels are not correct. The refocused beams trace out the trajectories shown in the diagram below the energy levels. It is seen that, for $A$ positive, the refocused beam goes around the obstacle wire on that side of the neutral axis which is closer to the convex pole piece of the $B$ magnet (i.e., with a transverse acceleration which is opposite in direction to the gradient in the $B$ field). The opposite is true in the case of $A$ negative. By moving the second obstacle wire to one side or the other of the neutral position, we have found that Fig. 6(a) holds, i.e., that $A$ is positive.

The use of two obstacle wires instead of the usual one is necessitated by the fact that there are in the beam many atoms of low effective magnetic moment or high velocity or both which are only slightly deflected by the $A$ and $B$ fields. If we tried to explore the trajectory of the atoms by the use of only one obstacle wire, we would find that these slightly deflected atoms would obscure the observations completely.

## V. EVALUATION OF THE NUCLEAR MOMENTS

### (a) Possibility of Magnetic Perturbation

The observed deviation from the interval rule has been ascribed to the existence of a nuclear electric quadrupole interaction. It is of interest to see whether such a deviation could arise from a magnetic perturbation by a neighboring fine structure level. Casimir[4] has calculated the effects of such a magnetic interaction. His conclusions are: that only levels with the same $J$ or with $J$'s differing by one perturb each other, that levels with the same $F$ repel each other, and that the repulsion between two levels with the total quantum number $F$ and electronic angular momenta $J$ and $J+1$ is given by

$$W=\frac{|(n,J;F|T|n',J+1;F)|^2}{W(n',J+1;F)-W(n,J;F)}, \tag{7}$$

where the denominator is the separation between the two hyperfine levels concerned (usually replaceable by the fine structure separation) and the numerator is given by

$$(n,J,F|T|n',J+1,F)$$
$$=-\gamma\frac{(n,J|H_z|n',J+1)_{m_J=J}}{(2J+1)^{\frac{1}{2}}}\tfrac{1}{2}[(F+J+I+2)$$
$$\times(F+J-I+1)(J+I+1-F)(F-J+1)]^{\frac{1}{2}}$$
$$\times 1.585\times 10^{-3}\ \text{cm}^{-1}. \tag{8}$$

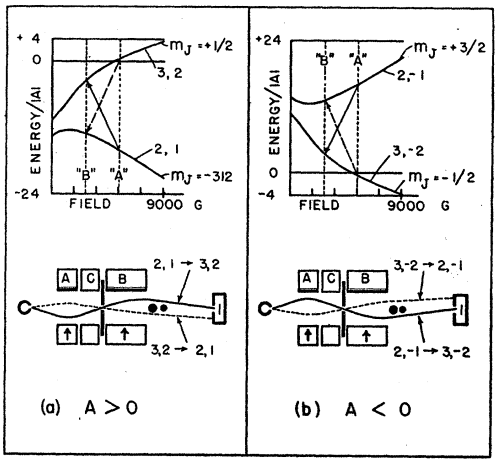


FIG. 6. Diagrams of energy levels used in the determination of the sign of $A$ and the trajectories of the atoms for $A$ positive and $A$ negative. The energy levels are taken from Fig. 1.

$\gamma$ is the positive ratio of the nuclear magnetic moment in nuclear magnetons to the nuclear spin in units of $h/2\pi$. In order to evaluate the matrix element of $H_z$ connecting the two perturbing states, it is necessary to know the eigenfunctions of the states. However, it is possible to find the relative displacements of levels of different $F$ belonging to the same fine structure multiplet without such knowledge.

An approximate picture of the $^4I$ fine structure multiplet of the $4f^36s^2$ ground configuration of Pr I may be deduced from the known ground levels of Pr II. According to Rosen, Harrison, and McNally,[2] the lowest terms of Pr II arise from a $4f^36s$ configuration and consist of four pairs of levels as shown in Fig. 7. This pattern is indicative of a strong $Jj$ coupling between the $s$ electron and the $f^3$ core. It can be shown on theoretical grounds that the lowest levels of the configuration $f^3$ or $f^3s^2$ would then consist of levels with spacings corresponding to the spacings of the centers of gravity of these pairs. This picture has been borne out in the $f^4s^2$, $^5I$ and $f^4s$, $^{6,4}I$ terms of NdI and NdII, respectively.[3] Thus, we find that the $^4I_{11/2}$ level of Pr I should lie at approximately 1450 $\text{cm}^{-1}$ above the $^4I_{9/2}$ level.

The hyperfine structure of $^4I_{11/2}$ consists of six levels with $F=8, 7, 6, 5, 4, 3$. All of these levels, except $F=8$, will repel the corresponding ones of $^4I_{9/2}$. Since our observations concern only the $F=4$ and $F=3$ levels, we shall consider only their relative displacements. Since the fine structure separation, by our estimate above, is about 1600 times the total hfs of $^4I_{9/2}$, we may replace the actual separation between the hyperfine levels required in Eq. (8) by the fine structure separation. Then, by Eqs. (7) and (8), the relative displacements are

$$\delta W(F=4)/\delta W(F=3)=91/45\simeq 2.$$

Calling the displacement downwards of the $F=3$ level

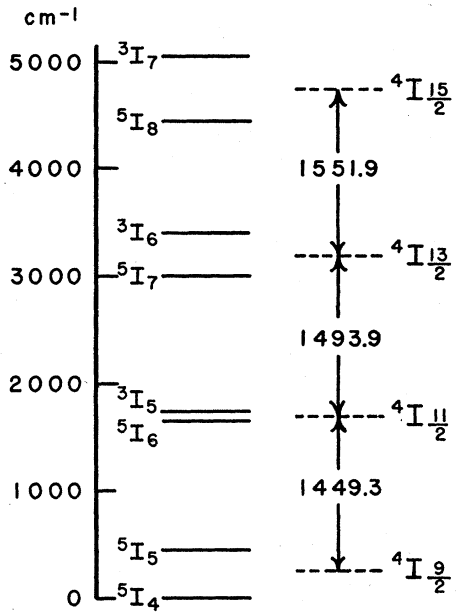


FIG. 7. The fine structure of the ground state of Pr II according to Rosen, Harrison, and MacNally. The separations between the centers of gravity of the pairs of lines give an estimate of the fine structure of the ground state of Pr I.

$\delta$, the displacement of the $F=4$ level is then $2\delta$, also downwards. If we assume that, without perturbation, the interval rule holds with the interval factor $A'$, we may write

$$4A'-\delta=3708.05, \quad 3A'-\delta=2782.25.$$

Solving for $\delta$, we obtain $\delta=-4.85$ Mc/sec. A negative value for $\delta$, however, means that the levels have been displaced upwards in contradiction to the original assumption of a mutual repulsion. An upward displacement would be consistent with a repulsion only if the $^4I_{11/2}$ level were below the $^4I_{9/2}$ level. Such an inverted fine structure cannot be the case, for otherwise we would have seen low frequency transitions in the hfs of $^4I_{15/2}$. Furthermore, it should not occur on theoretical grounds from the known structure of Pr II. We conclude then that the observed deviation cannot be entirely due to a perturbation and assume that, in the absence of further data, it is caused by a nuclear electric quadrupole moment. The magnetic dipole interaction constant $A$ and the nuclear electric quadrupole interaction constant $B$ are then as we have given them above.

### (b) The Nuclear Magnetic Dipole Moment

The interaction constant $A=926.03$ Mc/sec represents the resultant interaction of three equivalent $4f$ electrons with the nucleus. Since relativity can be neglected for $4f$ electrons, the contribution resulting from a single $4f$ electron may be calculated by a method attributable to Goudsmit.[17] We find

$$a_{4f}=+0.7626A(f^3, {}^4I_{9/2})=706.2 \text{ Mc/sec}.$$

There are a number of theoretical relations connecting this quantity with the gyromagnetic ratio of the nucleus, relations which involve varying assumptions about the field in which the electron moves. For simplicity, we have chosen the relation which assumes that the $4f$ electron moves in a hydrogen-like field. It is

$$a_{4f}=\frac{\gamma}{1836}\frac{R\alpha^2(Z-\sigma)^3}{n^3l(l+\frac{1}{2})(l+1)},$$

where $\gamma$ is as defined previously and $\sigma$ is a screening constant. A reasonable value of $\sigma$ may be obtained from the known fine structure of the $4f^46s^2\ {}^5I$ ground state of Nd I (see P. Schuurmanns[3]). The measured total width of this fine structure is 5048 cm$^{-1}$. Assuming that Russell-Saunders coupling applies, this width is also equal to $26\zeta$, where $\zeta$ is the Landé interval factor. Thus, $\zeta=194.15$ cm$^{-1}$. According to a relation in Condon and Shortley,[7] the contribution to $\zeta(4f^4, {}^5I)$ by a single $4f$ electron is $\zeta_{4f}=4\zeta$. Hence, $\zeta_{4f}=776.6$ cm$^{-1}$. If we again assume hydrogen-like wave functions for this electron, we may write

$$\zeta_{4f}=\frac{R\alpha^2(Z-\sigma)^4}{n^3l(l+\frac{1}{2})(l+1)}.$$

Substituting for the various quantities in this relation, we obtain $\sigma=35.5$. A value of 35.25 is obtained for $\sigma$, when we apply the same method to the estimated fine structure of Pr I. Using $\sigma=35.5$ in the expression for $a_{4f}$, we find the nuclear gyromagnetic ratio $\gamma=+1.53$. With $I=5/2$, the nuclear magnetic moment is

$$\mu=+3.8 \text{ nm}.$$

In view of the very approximate nature of the formulas which we have used in the evaluation of $\mu$, it would be desirable to have an independent estimate of the reliability of the procedure. To this end, we have applied our crude method to $Sc^{45}$, $V^{51}$, and $Cu^{63}$, the nuclear moments of which are known with high precision. The configurations $3d4s^2$, $3d^34s^2$ and $3d^94s^2$, respectively, of these elements are similar to that of Pr in that there is an $s^2$ closed shell outside of an incompletely filled shell. The terms we have used are the lowest ones of these configurations, namely, $^2D$, $^4F$, and $^2D$, respectively, with values taken from the National Bureau of Standards Atomic Energy Levels.[18] The hyperfine structure data are taken from the article of Brix and Kopfermann in Landolt-Börnstein.[19] We find by our method a value of $\mu$ for Sc which is 14 percent

[17] S. Goudsmit, Phys. Rev. **37**, 663 (1931).
[18] U. S. Department of Commerce, National Bureau of Standards Circular No. 467, Vol. I (1949) and Vol. II (1952).
[19] Landolt-Börnstein, *Zahlenwerte und Funktionen* (Verlag. Julius Springer, Berlin, 1952), sixth edition, Vol. I, Part 5.

too low, for V one 16 percent too high, and for Cu one 10 percent too high. Since the wave functions for the $3d$ electrons of these elements are probably not so hydrogen-like as that of the $4f$ electron of Pr, we take the lowest of the above errors, $\pm 10$ percent, as the estimated error of our value of $\mu$.

### (c) The Nuclear Electric Quadrupole Moment

According to Casimir, the interaction constant $B$, in $\text{sec}^{-1}$, is related to the nuclear electric quadrupole moment $Q$ through the relation

$$hB=-e^2Q\left\langle\frac{3\cos^2\theta_e-1}{r_e^3}\right\rangle_{J,J}.$$

In this relation, $h$ is Planck's constant, $e$ the electronic charge, $\theta_e$ and $r_e$ the coordinates of an element of charge in the electronic charge distribution. The expression in the angular brackets is to be averaged over the electronic state for which $m_J=J$. If we assume a central field approximation for the electronic state, we may separate the radial and angular parts of the wave function and write for the quadrupole moment

$$Q=-\frac{hB}{e^2\langle 3\cos^2\theta_e-1\rangle_{J,J}\langle 1/r_e^3\rangle_{J,J}}.$$

As in our evaluation of the magnetic dipole moment, we shall again assume hydrogenic wave functions and use the same $\langle 1/r_e^3\rangle$ as before, i.e.,

$$\left\langle\frac{1}{r_e^3}\right\rangle=\frac{(Z-\sigma)^3}{a_0^3n^3l(l+\frac{1}{2})(l+1)},$$

where $a_0$ is the radius of the first Bohr orbit in hydrogen.

To evaluate $\langle 3\cos^2\theta_e-1\rangle$ for the $^4I_{9/2}$, $m_J=9/2$ state, we adopt the procedure followed by Schmidt[20] in the calculation of the quadrupole moment of Ta. The wave function of $^4I_{9/2}$, $m_J=9/2$ is expressed as a sum of products of wave functions of the individual electrons. The matrix elements of $(3\cos^2\theta-1)$ for the individual electrons are evaluated by means of the Pauli wave functions for the electron. The details of the calculations are shown in the Appendix. The quantity finally obtained is

$$\langle {}^4I_{9/2}|3\cos^2\theta-1|{}^4I_{9/2}\rangle_{m_J=9/2}=-0.2314.$$

Using this and the above-mentioned substitution for $\langle 1/r^3\rangle$, we find for the nuclear quadrupole moment

$$Q=-0.054\times 10^{-24}\ \text{cm}^2.$$

### (d) Remarks on Nuclear Moments

In the calculation of the electronic quantities $\langle r_e^{-3}\rangle$ and $\langle 3\cos^2\theta_e-1\rangle$, we have assumed that Russell-Saunders coupling holds for the three $f$ electrons. Since, however, the exact coupling is not known, it is difficult to say how reliable the nuclear moments we have calculated are. The best indication we have is that our value of $\mu$ agrees well with the value of 3.9 nm obtained by Brix[21] from hfs spectra arising essentially from an $s$-electron. Since, in this case, the uncertainties concerning couplings between electrons are not present, we may conclude that the procedure we have followed is essentially correct and that our value of the magnetic moment of Pr is probably quite reliable. This value lies well within the Schmidt limits of magnetic moments calculated on the basis of an individual particle model of the nucleus and, in fact, lies on one of the "$B$" limits calculated by Bohr[22] on the assumption of a single particle moving in a nonspherically symmetric field.

A theoretical value for the quadrupole moment of Pr has been given by Van Wageningen and de Boer[23] who also used a spheroidal nuclear model. Their value of $-0.86\times 10^{-24}$ cm$^2$ agrees with ours in sign but is an order of magnitude greater. The negative sign of the experimental value tends to confirm the view that the moments of Pr arise mainly from a single proton outside of completed shells and subshells. As to the magnitude of the experimental value, it is difficult to estimate its accuracy. However, it may be pointed out that Schmidt[20] and Brown and Tamboulian,[24] using the same procedure, have obtained consistent values of the quadrupole moment of $Ta^{181}$ from different terms.

The atomic beam laboratory in which the present experiment was done is part of the Spectroscopy Laboratory of the Physics Division of the National Research Council of Canada. To Dr. G. Herzberg and Dr. A. E. Douglas of this laboratory the writer is very grateful for their continued encouragement and assistance throughout the construction of the atomic beam apparatus and the course of the experiment. The writer is also pleased to thank Dr. P. Brix for stimulating discussions on the evaluation of the nuclear moments.

## APPENDIX

### Evaluation of $(3\cos^2\theta-1)_{J,J}$

To evaluate the average value of $(3\cos^2\theta-1)$ for the $^4I_{9/2}$ state with $m_J=9/2$, we first seek an expression for the wave function of this state in terms of single electron wave functions. Let us denote the wave function of a state characterized by the weak-field quantum numbers $S$, $L$, $J$, $m_J$ by the spectroscopic symbol for the state itself, with the addition of a superscript for the value of $m_J$; thus, $^4I_{9/2}{}^{9/2}$ will denote the wave function of the state with $S=3/2$, $L=6$, $J=9/2$, $m_J=9/2$. Similarly, let us denote a wave function in the strong field or

[20] T. Schmidt, Z. Physik **121**, 63 (1943).

[21] P. Brix, Phys. Rev. **89**, 1245 (1953).

[22] A. Bohr, Phys. Rev. **81**, 134 (1951).

[23] R. Van Wageningen and J. de Boer, Physica **18**, 369 (1952).

[24] B. M. Brown and D. H. Tamboulian, Phys. Rev. **88**, 1158 (1952).

$(S, L, m_L, m_S)$-representation by the spectroscopic symbol for $S$ and $L$, followed by two subscripts giving $m_L$ and $m_S$; thus, ${}^4I_{6,-3/2}$ will denote the wave function of a state with $S=3/2$, $L=6$, $m_L=6$, $m_S=-3/2$. We may then expand ${}^4I_{9/2}{}^{9/2}$ in terms of strong field wave functions thus:

$$\begin{aligned}{}^4I_{9/2}{}^{9/2}=&(10/13)^{\frac{1}{2}}\,{}^4I_{6,-3/2}-\tfrac{1}{2}(10/13)^{\frac{1}{2}}\,{}^4I_{5,-1/2}\\&+(5/11\cdot13)^{\frac{1}{2}}\,{}^4I_{4,1/2}-(1/2\cdot11\cdot13)^{\frac{1}{2}}\,{}^4I_{3,3/2},\end{aligned}\quad\text{(A1)}$$

where the coefficients of the expansion may be found by the use of Table III[3] of Condon and Shortley.[7] The strong field wave functions are expressible by the method of Gray and Wills[25] in terms of products of wave functions of the individual $f$ electrons which give rise to these terms. We find, in the notation of Condon and Shortley,

$$\begin{aligned}{}^4I_{6,-3/2}&=(3^-2^-1^-),\\{}^4I_{5,-1/2}&=[(3^+2^-0^-)+(3^-2^+0^-)+(3^-2^-0^+)]/\sqrt{3},\\{}^4I_{4,1/2}&=[\sqrt{5}(3^+1^+0^-)+\sqrt{5}(3^+1^-0^+)+\sqrt{5}(3^-1^+0^+)\\&\quad+\sqrt{6}(3^+2^+-1^-)+\sqrt{6}(3^+2^--1^+)\\&\quad+\sqrt{6}(3^-2^+-1^+)]/\sqrt{(3\cdot11)},\\{}^4I_{3,3/2}&=[(2^+1^+0^+)+2\sqrt{2}(3^+1^+-1^+)\\&\quad+\sqrt{2}(3^+2^+-2^+)]/\sqrt{11}.\end{aligned}\quad\text{(A2)}$$

Combining Eqs. (A1) and (A2), we have an expression for ${}^4I_{9/2}{}^{9/2}$ in terms of single electron wave functions.

In order to evaluate $\langle {}^4I_{9/2}{}^{9/2}|3\cos^2\theta-1|{}^4I_{9/2}{}^{9/2}\rangle$, using the above expansion, we need to know the matrix elements of $(3\cos^2\theta-1)$ for strong field single electron wave functions, i.e., we need to know the value of such expressions as $\langle 2^+|\alpha|3^-\rangle$, where $\alpha\equiv3\cos^2\theta-1$. By the use of Pauli wave functions for the electron, we may write down the matrix elements of $\alpha$ in the $(s, l, j, m)$ or weak field representation. The desired matrix elements of $\alpha$ in the $(s, l, m_s, m_l)$ or strong field representation will then be obtained by applying the standard transformation between these two representations.

Denoting the wave function of an electron with quantum numbers $s$, $l$, $j$, $m$ by $l_j{}^m$, the following expressions can easily be derived using Pauli wave functions:

$$\langle l_{j=l\pm\frac{1}{2}}{}^m|\alpha|l_{j=l\pm\frac{1}{2}}{}^m\rangle=-\frac{1}{2}\frac{3m^2-j(j+1)}{j(j+1)},$$

$$\langle l_{j=l+\frac{1}{2}}{}^m|\alpha|l_{j=l-\frac{1}{2}}{}^m\rangle=\frac{12m[(l+\frac{1}{2}+m)(l+\frac{1}{2}-m)]^{\frac{1}{2}}}{(2l-1)(2l+1)(2l+3)}.$$

Into these expressions may be introduced the relativistic correction factors given in Casimir,[4] $R'$ in the diagonal matrix elements with $j=l+\frac{1}{2}$, $R''$ in the diagonal matrix elements with $j=l-\frac{1}{2}$, and $S$ in the nondiagonal matrix elements. Thus, for an $f$ electron, we have the following weak field matrix elements:

$$\begin{aligned}&\langle f_{7/2}{}^{\pm7/2}|\alpha|f_{7/2}{}^{\pm7/2}\rangle=-\tfrac{2}{3}R',\\&\langle f_{5/2}{}^{\pm5/2}|\alpha|f_{5/2}{}^{\pm5/2}\rangle=-4R''/7,\\&\langle f_{7/2}{}^{\pm5/2}|\alpha|f_{7/2}{}^{\pm5/2}\rangle=-2R'/21,\\&\langle f_{5/2}{}^{\pm3/2}|\alpha|f_{5/2}{}^{\pm3/2}\rangle=4R''/35,\\&\langle f_{7/2}{}^{\pm3/2}|\alpha|f_{7/2}{}^{\pm3/2}\rangle=+2R'/7,\\&\langle f_{5/2}{}^{\pm1/2}|\alpha|f_{5/2}{}^{\pm1/2}\rangle=16R''/35,\\&\langle f_{7/2}{}^{\pm1/2}|\alpha|f_{7/2}{}^{\pm1/2}\rangle=+10R'/21,\\&\langle f_{7/2}{}^{5/2}|\alpha|f_{5/2}{}^{5/2}\rangle=-\langle f_{7/2}{}^{-5/2}|\alpha|f_{5/2}{}^{-5/2}\rangle=2(6)^{\frac{1}{2}}S/21,\\&\langle f_{7/2}{}^{3/2}|\alpha|f_{5/2}{}^{3/2}\rangle=-\langle f_{7/2}{}^{-3/2}|\alpha|f_{5/2}{}^{-3/2}\rangle=2(10)^{\frac{1}{2}}S/35,\\&\langle f_{7/2}{}^{1/2}|\alpha|f_{5/2}{}^{1/2}\rangle=-\langle f_{7/2}{}^{-1/2}|\alpha|f_{5/2}{}^{-1/2}\rangle=4(3)^{\frac{1}{2}}S/105.\end{aligned}$$

The transformation of these matrix elements to the $(m_l, m_s)$ scheme is done in a straightforward manner following the choice of phase factors specified on page 123 of Condon and Shortley. We find:

$$\begin{aligned}&\langle3^+|\alpha|3^+\rangle=\langle-3^-|\alpha|-3^-\rangle=-\tfrac{2}{3}R',\\&\langle3^-|\alpha|3^-\rangle=\langle-3^+|\alpha|-3^+\rangle\\&\qquad=-(2/147)(R'+36R''+12S),\\&\langle2^+|\alpha|2^+\rangle=\langle-2^-|\alpha|-2^-\rangle=-(12/147)(R'+R''-2S),\\&\langle2^-|\alpha|2^-\rangle=\langle-2^+|\alpha|-2^+\rangle=(20/245)(R'+R''-2S),\\&\langle1^+|\alpha|1^+\rangle=\langle-1^-|\alpha|-1^-\rangle\\&\qquad=(2/245)(25R'+4R''+20S),\\&\langle1^-|\alpha|1^-\rangle=\langle-1^+|\alpha|-1^+\rangle\\&\qquad=(2/245)(25R'+32R''-8S),\\&\langle0^+|\alpha|0^+\rangle=\langle0^-|\alpha|0^-\rangle=(8/735)(25R'+18R''+6S),\\&\langle3^-|\alpha|2^+\rangle=\langle-2^-|\alpha|-3^+\rangle\\&\qquad=-(2\sqrt{6}/147)(R'-6R''+5S),\\&\langle2^-|\alpha|1^+\rangle=\langle-1^-|\alpha|-2^+\rangle\\&\qquad=(2\sqrt{10}/245)(5R'-2R''-3S),\\&\langle1^-|\alpha|0^+\rangle=\langle0^-|\alpha|-1^+\rangle=(4\sqrt{3}/735)(25R'-24R''-\mathrm{S}).\end{aligned}$$

These matrix elements are now substituted into the expanded form of $\langle {}^4I_{9/2}{}^{9/2}|3\cos^2\theta-1|{}^4I_{9/2}{}^{9/2}\rangle$. The evaluation of the expansion is facilitated by the application of the results of section 6[6] of Condon and Shortley. The final expression obtained is

$$\begin{aligned}&\langle {}^4I_{9/2}{}^{9/2}|3\cos^2\theta-1|{}^4I_{9/2}{}^{9/2}\rangle\\&\quad=(92\,820R'-6552R''-353\,808S)/1\,156\,155.\end{aligned}$$

If we let $R'=R''=S=1$, thus neglecting relativistic corrections, we get

$$\langle3\cos^2\theta-1\rangle_{J,J}=-0.2314.$$

[25] N. M. Gray and L. A. Wills Phys. Rev. **38**, 248 (1931).